THE JOURNAL OF BIOLOGICAL CHEMISTRY VOL. 286, NO. 1, pp. 199–207, January 7, 2011

Rac GTPase-activating Protein (Rac GAP) α1-Chimaerin Undergoes Proteasomal Degradation and Is Stabilized by Diacylglycerol Signaling in Neurons*

Received for publication, July 21, 2010, and in revised form, October 12, 2010 Published, JBC Papers in Press, November 5, 2010, DOI 10.1074/jbc.M110.166728

Jamie R. K. Marland, DingXin Pan, and Philip C. Buttery[1]

From the Centre for Brain Repair, University of Cambridge, Cambridge CB2 0PY, United Kingdom

α1-Chimaerin is a neuron-specific member of the Rho GTPase-activating protein family that selectively inactivates the small GTPase Rac. It is known to regulate the structure of dendrites and dendritic spines. We describe here that under basal conditions α1-chimaerin becomes polyubiquitinated and undergoes rapid proteasomal degradation. This degradation is partly dependent on the N-terminal region that is unique to this isoform. Mimicking diacylglycerol (DAG) signaling with a phorbol ester stabilizes endogenous α1-chimaerin against degradation and causes accumulation of the protein. The stabilization requires phorbol ester binding via the C1 domain of the protein and is independent of PKC activity. In addition, overexpression of a constitutively active Rac1 mutant is sufficient to cause an accumulation of α1-chimaerin through a phospholipase C-dependent mechanism, showing that endogenous DAG signaling can also stabilize the protein. These results suggest that signaling via DAG may regulate the abundance of α1-chimaerin under physiological conditions, providing a new model for understanding how its activity could be controlled.

Dendritic spines are the post-synaptic component of most excitatory synapses in the central nervous system and exhibit a large degree of structural plasticity (1). The actin cytoskeleton is highly enriched within spines, acting both as a structural support and driver of morphological change (2). Members of the Rho small GTPase family control the dynamics of actin through a complex set of downstream effectors (3), and in neurons the family member Rac1 is closely involved in regulating spine structure and density (4, 5).

Two groups of proteins have important roles in Rho GTPase regulation; their signaling is activated by guanine nucleotide exchange factors, which promote formation of the active GTP-bound form, whereas GTPase-activating proteins (GAPs)[2] increase the level of the inactive GDP-bound form by accelerating hydrolysis of GTP (3). In previous work, we found that the neuron-specific Rac GAP α1-chimaerin regulates spine and dendrite morphology through a mechanism that depends on its GAP activity. We showed that overexpression of α1-chimaerin in neurons causes spine pruning, whereas knockdown promotes overgrowth of atypical spines and filopodia from dendrites (6). These effects suggest α1-chimaerin has a role in the maintenance of normal spine structure.

Vertebrate genomes contain two chimaerin genes: *CHN1* encodes the α-chimaerins, and *CHN2* encodes the β-chimaerins, with each gene giving rise to two alternative transcripts that are translated into proteins differing at their N termini (7). α1- and β1-chimaerin have a relatively short N-terminal region that does not encode any recognizable domains, whereas α2- and β2-chimaerin both include a functional SH2 domain that can bind to phosphotyrosine motifs within receptors such as EphA4 (8–12). All chimaerin isoforms contain a GAP domain with specificity *in vitro* for Rac1 (13, 14), and they are unique among other Rho GAPs because they also contain a diacylglycerol (DAG)-binding C1 domain, more commonly associated with members of the protein kinase C (PKC) family (15). DAG is a lipid second messenger produced at cell membranes from phosphatidylinositol 4,5-bisphosphate by members of the phospholipase C (PLC) family in response to a wide variety of stimuli. The C1 domain allows chimaerins to translocate to membranes in response to DAG signaling (6, 16) and is likely to anchor them in close proximity to activated Rac.

It is becoming clear that the SH2 domain is central to the regulation of α2- and β2-chimaerin activity, as under unstimulated conditions it folds over and occludes the C1 and GAP domains, auto-inhibiting the whole molecule (17–19). However, because α1-chimaerin lacks this SH2 domain, it is not clear how its activity is regulated. Because accurate control of Rac activation is essential for maintaining normal neuronal structure, we hypothesized that other mechanisms would also exist to finely regulate α1-chimaerin within these cells. We show here that the abundance of α1-chimaerin in neurons is actively controlled by proteasomal degradation and selective stabilization following DAG signaling, suggesting a novel means by which α1-chimaerin activity may be regulated.

EXPERIMENTAL PROCEDURES

Reagents, Antibodies, and Drugs—Unless otherwise noted, all general reagents were obtained from Sigma; cell culture

* This work was supported by an Alzheimer's Research Trust pilot grant (to P. C. B.) and by a Medical Research Council studentship (to J. R. K. M.).

[1] To whom correspondence should be addressed: Cambridge Centre for Brain Repair, ED Adrian Bldg., Forvie Site, Robinson Way, Cambridge, CB2 0PY, United Kingdom. Tel.: 44-1223-331160; Fax: 44-1223-331174; E-mail: pcb10@cam.ac.uk.

[2] The abbreviations used are: GAP, GTPase-activating protein; SH2, Src homology 2; DAG, diacylglycerol; PLC, phospholipase C; CHX, cycloheximide; NTR, N-terminal region; PMA, phorbol 12-myristate 13-acetate; EGFP, enhanced green fluorescent protein; CI, confidence interval; FL, full-length; HA3, triple hemagglutinin; BisTris, 2-[bis(2-hydroxyethyl)-amino]-2-(hydroxymethyl)propane-1,3-diol.

reagents were from Invitrogen, and drugs were from Merck. Polyclonal rabbit anti-α1-chimaerin antibody was a gift from P. Scheiffele (University of Basel), and its production and characterization have been described before (6). This antibody produces a background band when used for Western blotting; for clarity this is not shown in the figures. Other antibodies were from commercial sources as follows: rat monoclonal anti-HA 3F10 (Roche Applied Science); mouse monoclonal anti-β-actin AC-15 (Sigma); mouse monoclonal anti-ubiquitin P4D1-A11 (Millipore); mouse monoclonal anti-HA 16B12 (Covance); rabbit polyclonal anti-GFP (Invitrogen); mouse monoclonal anti-GFP 3E6 (Invitrogen), and rabbit polyclonal anti-phospho-myristoylated alanine-rich C kinase substrate (Ser-152/156) (Cell Signaling Technology). MG132 and clasto-lactacystin β-lactone were dissolved in DMSO and used at 10 μM; cycloheximide was dissolved in ethanol and used at 200 μg/ml; phorbol 12-myristate 13-acetate was dissolved in DMSO and used at 2 μM; and Ro 31-8220 was dissolved in DMSO and used at 2 μM. Solvent-only controls were used wherever appropriate, and the total DMSO concentration in culture medium never exceeded 0.2%.

Cell Culture and Transfection—293 cells were grown as monolayer cultures in Dulbecco's modified Eagle's medium (DMEM) supplemented with 10% heat-inactivated fetal calf serum (FCS), 100 units/ml penicillin, 100 μg/ml streptomycin, and 0.25 μg/ml amphotericin B. Primary hippocampal neuron cultures were generated using a protocol based on previously described techniques (20), with some modifications. Hippocampal tissue from Sprague-Dawley rat embryos (Charles River) at day 18 of gestation was collected in Hanks' buffered saline solution (Ca^{2+}- and Mg^{2+}-free) and then digested in 0.25% trypsin for 15 min at 37 °C followed by gentle trituration using a fire-polished glass pipette. This produced a single cell suspension that was diluted into warmed DMEM supplemented with 10% FCS and an additional 0.8% glucose and then plated at a density of 1×10^5 viable cells/well into 24-well tissue culture plates (Nunc) coated with 250 μg/ml poly-D-lysine (30–70 kDa, Sigma). The cultures were incubated for 4 h to allow cell attachment, and then the medium was changed to Neurobasal supplemented with 2% B27 and 1% GlutaMAX. Unused spaces within the plates were filled with sterile water to minimize evaporation, and 50% of the medium was changed every 7 days to promote long term cell survival. All neuronal cultures were grown for 18–22 days in a tissue culture incubator at 37 °C with a humidified 7% CO_2/air atmosphere before being used in experiments. Cells were transfected with plasmid DNA using Lipofectamine 2000 (Invitrogen) according to the manufacturer's instructions, and an equal mass of DNA was used in each transfection condition.

Plasmid Construction—EGFP was expressed from pEGFPN1 (Clontech). Plasmids encoding Rac1 wild type, Q61L, and T17N, all tagged at their N-terminal with EGFP, were a gift from M. R. Philips (New York University School of Medicine), and their construction has been described before (21, 22). HA3-tagged constructs were made using the pCAGGS/ES backbone (23, 24), which contains a chicken β-actin promoter to drive transcription and an expanded multiple cloning site. Annealed oligonucleotides encoding a triple repeat of the HA antigen (YPYDVPDYA) followed by a stop codon were inserted between the KpnI and SacI sites at the 3′ end of the pCAGGS/ES multiple cloning site to create pCHA3. Full-length (FL) and N-terminally truncated (ΔN58) α1-chimaerin were isolated as PCR products amplified from IMAGE Clone ID 7315609 (25), which contains full-length *Rattus norvegicus* α1-chimaerin. The primers introduced a Kozak consensus sequence and also NotI- and XhoI-cloning sites. Products were inserted between these sites in pCHA3 to create C-terminal fusions with HA3. Point mutations P91A and C114A were made using a QuikChange Lightning kit (Stratagene), following the manufacturer's instructions, with the original IMAGE clone as a template. The resulting point mutants were propagated and sequenced, and clones carrying the appropriate mutations were used as templates for subcloning into pCHA3 as above. The N-terminal region (N58) of α1-chimaerin was isolated by PCR from the original IMAGE clone. The primers introduced a Kozak consensus sequence, and BamHI and HindIII cloning sites, and the product was inserted into pEGFPN1 using these sites to create a C-terminal fusion with EGFP. All plasmids were sequenced to confirm their identity. Full details of inserted oligonucleotides and primers used to create these plasmids are available upon request.

SDS-PAGE and Western Blotting—Cells were lysed on ice in chilled RIPA buffer (50 mM Tris, pH 7.4, 1% IGEPAL CA-630, 0.25% sodium deoxycholate, 0.1% SDS, 150 mM NaCl, 1 mM EDTA) supplemented with MiniComplete EDTA-free protease inhibitors (Roche Applied Science) and also 1 mM NaF and 1 mM Na_3VO_4 if protein phosphorylation was being examined. Lysates were cleared of insoluble material by centrifugation at 18,000 × *g* for 10 min at 4 °C, and for examination of total protein, the whole cell lysates were sonicated using a Soniprep 150 (MSE) to reduce sample viscosity.

Samples were denatured by heating to 95 °C for 10 min in reducing LDS sample buffer (Invitrogen), separated by electrophoresis using a BisTris-based SDS-PAGE system (26), and then transferred to Hybond P PVDF membrane (GE Healthcare). Proteins were detected by Western blotting, and antibody binding was detected by chemiluminescence using ECL Plus substrate and Hyperfilm ECL (both from GE Healthcare). Films were scanned on a flatbed scanner with image gamma set to 1.0 (linear response), and bands were quantified using the Gel Analyzer module of ImageJ (National Institutes of Health).

Cellular Ubiquitination Assay—293 cells were transfected with pCHA3-α1-chimaerin and treated the following day with 10 μM MG132 for 2 h. Cells were lysed on ice in chilled RIPA buffer supplemented with protease inhibitors and 10 mM *N*-ethylmaleimide to inhibit deubiquitination. After centrifugation of the lysate to remove insoluble material, 50 μg of protein was diluted with lysis buffer (containing inhibitors as above) to 1 ml and pre-cleared with nProtein G-Sepharose 4 Fast Flow (GE Healthcare) for 1 h at 4 °C. HA-tagged proteins were immunoprecipitated from the supernatant by incubation with 0.5 μg of rat monoclonal anti-HA for 2 h at 4 °C, followed by antibody capture with nProtein G-Sepharose 4 Fast

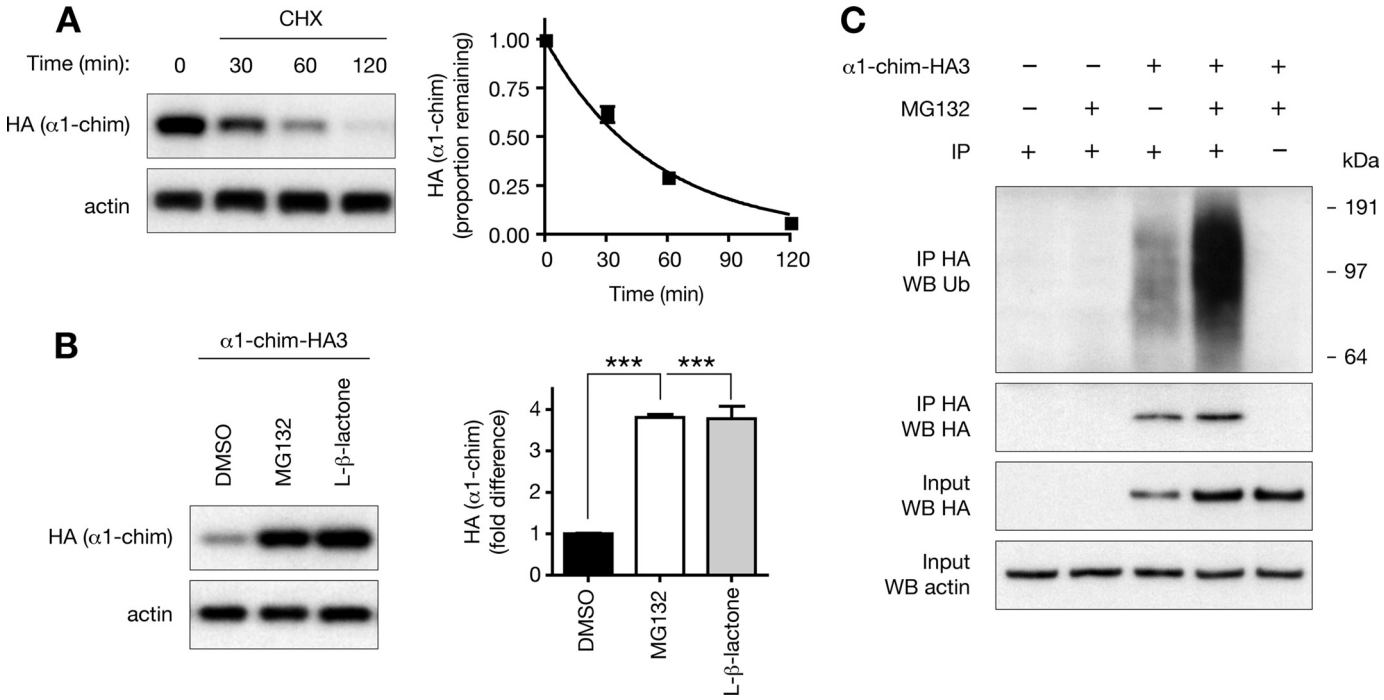

FIGURE 1. **α1-Chimaerin protein degradation in 293 cells.** *A*, 293 cells were transfected with α1-chimaerin-HA3 and treated with CHX (200 μg/ml) for the indicated times and then analyzed by Western blotting. *Left panel*, representative blots; *right panel*, densitometric analysis of α1-chimaerin-HA3 abundance, expressed as a proportion of the starting level ($n = 3$). *B*, 293 cells were transfected with α1-chimaerin-HA3, treated with the indicated drugs (both at 10 μM for 4 h) or DMSO, and then analyzed by Western blotting. *Left panel*, representative blots; *right panel*, densitometric analysis of α1-chimaerin-HA3 abundance, expressed as a proportion of the DMSO treated level ($n = 3$; ***, $p < 0.001$). *C*, 293 cells were transfected with α1-chimaerin-HA3 and treated with MG132 (10 μM for 2 h) as indicated and then lysed. HA-tagged proteins were immunoprecipitated (*IP*) from the lysates and analyzed by Western blotting (*WB*). *Ub*, ubiquitin.

Flow. The beads were thoroughly washed with cold RIPA buffer, and bound proteins were eluted and denatured by heating in reducing LDS sample buffer and then subjected to SDS-PAGE as described above.

Quantitative Immunofluorescence—Hippocampal neurons were grown on nitric acid-washed coverslips for 17–21 days, transfected as described in the text, and fixed 1–2 days later with 4% paraformaldehyde in phosphate-buffered saline (PBS) for 10 min at room temperature. Coverslips were blocked with 5% donkey serum in PBS containing 0.1% Triton X-100 (PBST) for 1 h, incubated for 1 h with primary antibodies diluted in 2% donkey serum/PBST, and then thoroughly washed in PBST. Primary antibody binding was detected by incubation for 30 min with Alexa-488- or Alexa-594-conjugated donkey secondary antibodies (Invitrogen) diluted in 2% donkey serum/PBST. Coverslips were then washed again in PBST and mounted on slides with FluorSave (Calbiochem). Images were acquired on a Leica DM6000 B wide field fluorescence microscope equipped with a Leica DFC350FX camera, using a 63× 1.40–0.60 NA (set at 1.0 NA) plan apochromatic oil immersion objective. Image acquisition settings were kept constant between imaging sessions to allow direct comparison of data. At least 20 images were taken of stained neurons from two coverslips per condition for each experimental repeat, and data from three repeats were combined for presentation and analysis. ImageJ was used to quantify the images by manually tracing the outline of each cell body and then using the program to calculate the mean fluorescence intensity for the appropriate channel within the traced area.

Statistics and Data Analysis—Data are presented as mean values ± S.E., unless otherwise stated. Selected differences between conditions were compared using two-tailed unpaired *t* tests. Protein half-lives were calculated by nonlinear regression with a one-component exponential decay model in Prism (GraphPad Software), using span = 1, K > 0, and plateau = 0 as constraints.

RESULTS

α1-Chimaerin Protein Is Degraded by the Ubiquitin-Proteasome System—Cells can actively regulate protein expression levels by targeted degradation. To explore whether α1-chimaerin might be regulated by this type of mechanism, we transfected 293 cells with α1-chimaerin tagged at its C terminus with an HA3 tag (α1-chimaerin-HA3), and we measured the half-life of the protein by blocking protein synthesis with cycloheximide (CHX) to reveal the rate of degradation. The amount of α1-chimaerin-HA3 remaining at several time points was assessed by Western blotting, and we found that α1-chimaerin-HA3 was rapidly lost, with a half-life of 36 min (95% CI, 33–41 min) (Fig. 1*A*).

The proteasome is a major site of cytosolic protein degradation in healthy cells. We tested whether it mediates α1-chimaerin degradation by transfecting 293 cells with α1-chimaerin-HA3 and inhibiting proteasome activity using MG132 or clasto-lactacystin β-lactone. Both drugs caused an accumulation of α1-chimaerin-HA3 (Fig. 1*B*), suggesting that the proteasome is involved in its degradation.

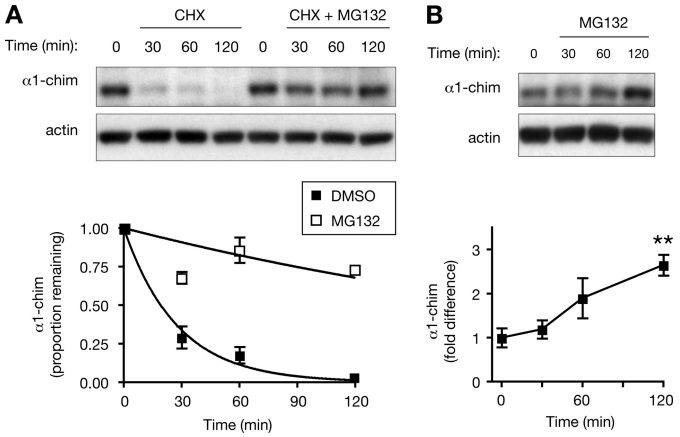

FIGURE 2. **α1-Chimaerin protein degradation in cultured neurons.** *A*, cultured neurons were treated with CHX (200 μg/ml) in the presence of MG132 (10 μM) or DMSO for the indicated times and then analyzed by Western blotting. *Upper panel*, representative blots; *lower panel*, densitometric analysis of α1-chimaerin abundance, expressed as a proportion of the starting levels ($n = 3$). *B*, cultured neurons were treated with MG132 (10 μM) for the indicated times and then analyzed by Western blotting. *Upper panel*, representative blots; *lower panel*, densitometric analysis of α1-chimaerin abundance, expressed as a proportion of the starting level ($n = 3$; **, $p < 0.01$).

However, an alternative possibility is that the proteasome degrades an intermediate stabilizing factor that prevents α1-chimaerin from being broken down by a nonproteasomal route. We therefore examined whether α1-chimaerin could become polyubiquitinated, a common modification of proteasome substrates. 293 cells were transfected with α1-chimaerin-HA3, and proteasomal degradation was inhibited with MG132 to promote accumulation of polyubiquitinated proteins. α1-Chimaerin-HA3 was immunoprecipitated from the cellular lysate and analyzed by Western blotting. We found that polyubiquitinated proteins were present at high molecular weights in the precipitated material from transfected cells and that this signal increased with MG132 treatment (Fig. 1*C*). This suggests that α1-chimaerin can be polyubiquitinated and targeted directly for degradation by the proteasome.

To investigate whether endogenous α1-chimaerin undergoes the same process, we used cultured mature hippocampal neurons, as the protein is expressed in these cells *in vivo*. The half-life of α1-chimaerin was again measured by blocking protein synthesis with CHX to reveal the rate of degradation by Western blotting. We observed that α1-chimaerin was rapidly lost, with a half-life of 19 min (95% CI, 16–25 min), suggesting that rapid degradation is a common feature of both overexpressed and endogenous α1-chimaerin (Fig. 2*A*). To test whether the proteasome is also responsible for α1-chimaerin degradation in neurons, we inhibited proteasome activity with MG132. In treated cultures, α1-chimaerin was stabilized against degradation, with its half-life increasing to 214 min (95% CI, 137–492 min) (Fig. 2*A*). Correspondingly, inhibition of proteasomal degradation in the absence of CHX caused an accumulation of endogenous α1-chimaerin in neurons (Fig. 2*B*).

Isoform-specific Sequences Are Involved in α1-Chimaerin Degradation—The α-chimaerins differ at their N termini, with α1-chimaerin containing a short and apparently unstructured N-terminal region (NTR), whereas α2-chimaerin contains a functional SH2 domain. To investigate whether the unique α1-chimaerin sequence regulates its degradation, we constructed a truncated mutant lacking the α1-chimaerin-specific NTR (ΔN58), tagged at its C terminus with an HA3 tag to avoid interfering with any functional sequences at the N terminus.

Neurons were co-transfected with either the FL or ΔN58 α1-chimaerin-HA3 and a second plasmid expressing EGFP so that transfected cells could later be identified using an unbiased marker. The relative stabilities of FL and ΔN58 α1-chimaerin were measured by examining abundance of the HA3 tag by quantitative immunofluorescence in transfected neurons across several time points after blocking protein synthesis with CHX. As expected, FL α1-chimaerin was rapidly lost, with a half-life of 33 min (95% CI, 26–44 min), whereas the truncated mutant was more stable with a half-life of 117 min (95% CI, 90–168 min), representing a 3.5-fold increase (Fig. 3*A*). This finding suggests that the unique α1-chimaerin NTR contributes to the rapid degradation of the protein, although other regions are also likely to be involved, because the truncated mutant still underwent a slow degradation when compared with α1-chimaerin in MG132 treated neurons (Fig. 2*A*).

We then tested whether the NTR is sufficient to direct the proteasomal degradation of a heterologous protein by using EGFP modified to carry the α1-chimaerin NTR at its N terminus (N58-EGFP). We expressed both EGFP and N58-EGFP in 293 cells and assessed the half-life of each protein by blocking protein synthesis with CHX. Western blotting showed that unmodified EGFP appeared to be extremely stable with a half-life of 1.5 days, whereas the complete N58-EGFP protein was rapidly degraded, with a half-life of 77 min (95% CI, 69–86 min) (Fig. 3*B*). The N58-EGFP appeared to be expressed in three forms with different molecular weights, most likely due to alternative translation from start sites downstream of the correct initiation codon. By using an antibody that recognizes first 14 residues of α1-chimaerin, we confirmed that the higher molecular weight band represented the complete fusion protein. Importantly, the proteasome inhibitor MG132 significantly blocked the degradation of the full-length fusion protein N58-EGFP (Fig. 3*C*), suggesting the α1-chimaerin NTR contains a sequence that specifically targets the protein for proteasomal degradation.

PMA Stimulation Stabilizes α1-Chimaerin and Causes It to Accumulate—The targeted nature of α1-chimaerin degradation suggested it might be a regulated process, forming a mechanism for actively controlling abundance of the protein. Because all chimaerin isoforms contain a DAG-binding C1 domain, we tested whether application of the artificial C1 domain ligand PMA could influence the degradation rate of α1-chimaerin. The protein half-life was tested as above, by blocking protein synthesis and measuring protein loss by Western blotting. We found that treatment of cultured neurons with PMA slowed the loss of α1-chimaerin in the presence of CHX, with a significant increase in half-life from 23 min (95% CI, 21–25 min) to 168 min (95% CI, 108–382 min) (Fig. 4*A*). This result shows a DAG-signaling mimetic causes α1-chimaerin to be stabilized against proteasomal degradation. Con-

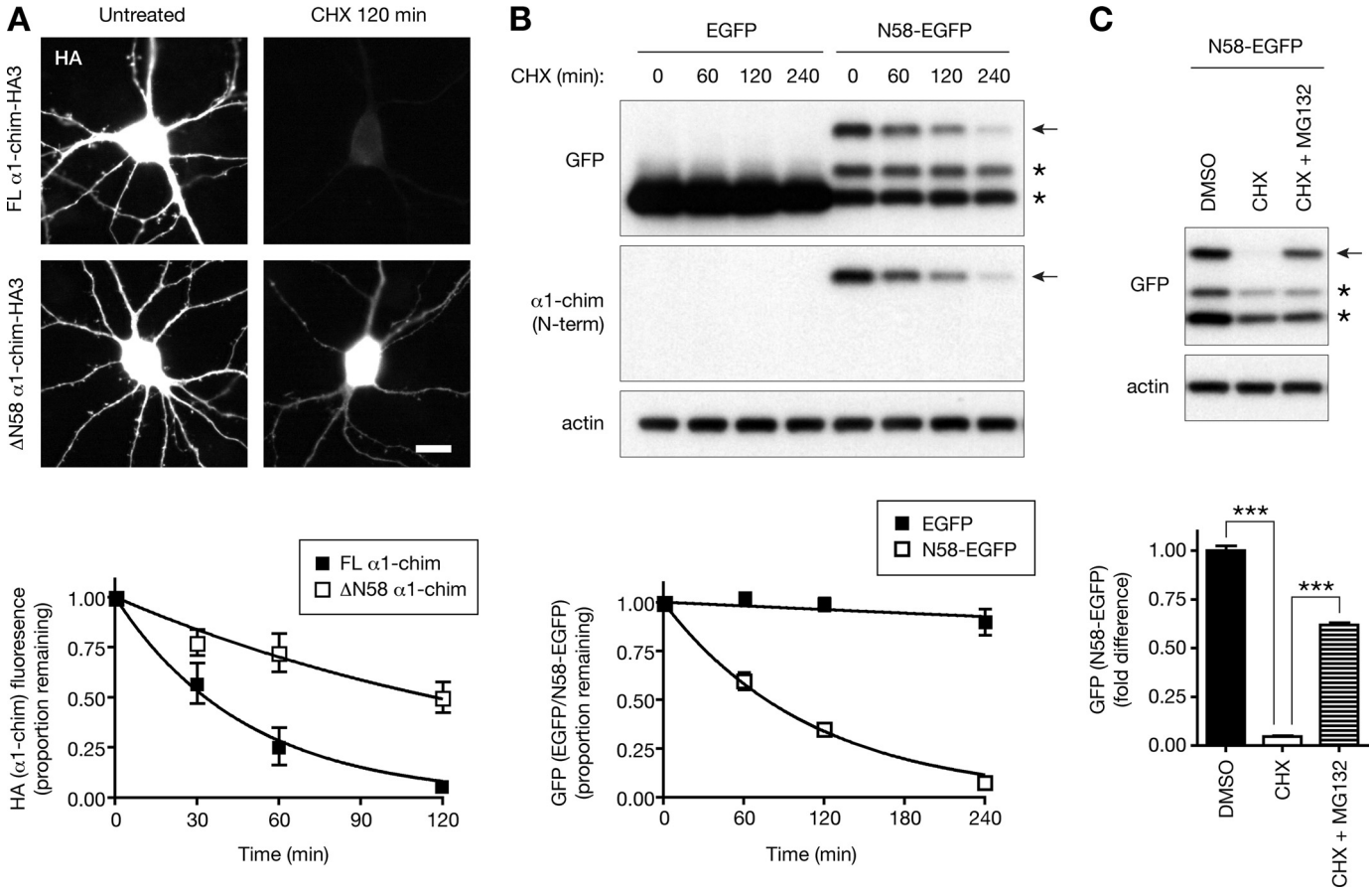

FIGURE 3. **Functional analysis of the α1-chimaerin N-terminal region.** *A*, cultured neurons were co-transfected with EGFP as a transfection marker and either FL or N-terminally truncated (ΔN58) α1-chimaerin-HA3. Cultures were treated with CHX (200 μg/ml), and then fixed and immunostained. *Upper panel*, representative images of HA staining in neurons transfected and treated as indicated (*scale bar* = 10 μm); *lower panel*, mean HA fluorescence intensities from neurons following treatment with CHX for the indicated times, expressed as a proportion of the starting intensity for each construct (20 neurons/experiment for each condition, $n = 3$ experiments). *B*, 293 cells were transfected with EGFP or N58-EGFP and treated with CHX (200 μg/ml) for the indicated times and then analyzed by Western blotting. *Upper panel*, representative blots showing expression of EGFP and fusion protein N58-EGFP (*arrow*), with truncated forms (*asterisks*) presumed to represent alternate start sites; blots are probed with either anti-GFP or anti-α1-chimaerin N-terminal antibody; *lower panel*, densitometric analysis of EGFP and complete N58-EGFP abundance, expressed as a proportion of the starting level ($n = 3$). *C*, 293 cells were transfected with N58-EGFP and treated with DMSO or CHX (200 μg/ml) alone or in combination with MG132 (10 μM) for 4 h. *Upper panel*, representative blots; *lower panel*, densitometric analysis of N58-EGFP abundance, expressed as a proportion of the DMSO treated level ($n = 3$; ***, $p < 0.001$).

sistent with this finding, we observed that treatment of neurons for 2 h with PMA alone caused a robust and significant accumulation of the protein, whereas the inactive phorbol ester isomer 4α-phorbol-12,13-didecanoate failed to produce any change (Fig. 4*B*).

PMA is not only bound by α1-chimaerin but also by many other proteins that contain C1 domains, including members of the PKC family. This raises the possibility that PMA could be acting via PKC. We therefore assessed the effect of PKC inhibition on α1-chimaerin stabilization by PMA, using the pan-PKC inhibitor Ro 31-8220. This inhibitor caused no change in α1-chimaerin accumulation following PMA exposure, but it blocked phosphorylation of the known PKC target myristoylated alanine-rich C kinase substrate (27), confirming its effectiveness (Fig. 4*C*). This shows that the stabilizing effect of PMA does not require PKC activity.

PMA Stabilizes α1-Chimaerin by Acting through the C1 Domain—To investigate whether PMA was instead acting directly on α1-chimaerin, we used versions carrying different point mutations within the C1 domain that are known to cause loss of phorbol ester binding. We have previously observed that α1-chimaerin bearing a C114A mutation fails to translocate in neurons following PMA application (6), and mutations of this residue have also been shown to prevent phorbol ester binding in biochemical assays (28). However, this mutation causes loss of binding by disrupting Zn^{2+} chelation within the C1 domain and is therefore likely to prevent correct folding of the tertiary structure of the domain; this may trigger the entire protein to be constitutively degraded by mechanisms that remove damaged and misfolded proteins. We therefore also created a version containing a P91A mutation, which strongly reduces the affinity of the C1 domain for phorbol esters (28) and prevents translocation in response to PMA, while avoiding disruption to the overall domain structure (18). The ability of PMA to stabilize these C1 domain point mutants was tested in neurons by co-transfecting them as HA3-tagged constructs in combination with EGFP as a transfection marker. After stimulation with PMA, the cells were analyzed by quantitative immunofluorescence for the HA epitope. The wild type protein accumulated as expected, whereas the P91A and C114A point mutants displayed significantly less accumulation following PMA stimulation (Fig. 5).

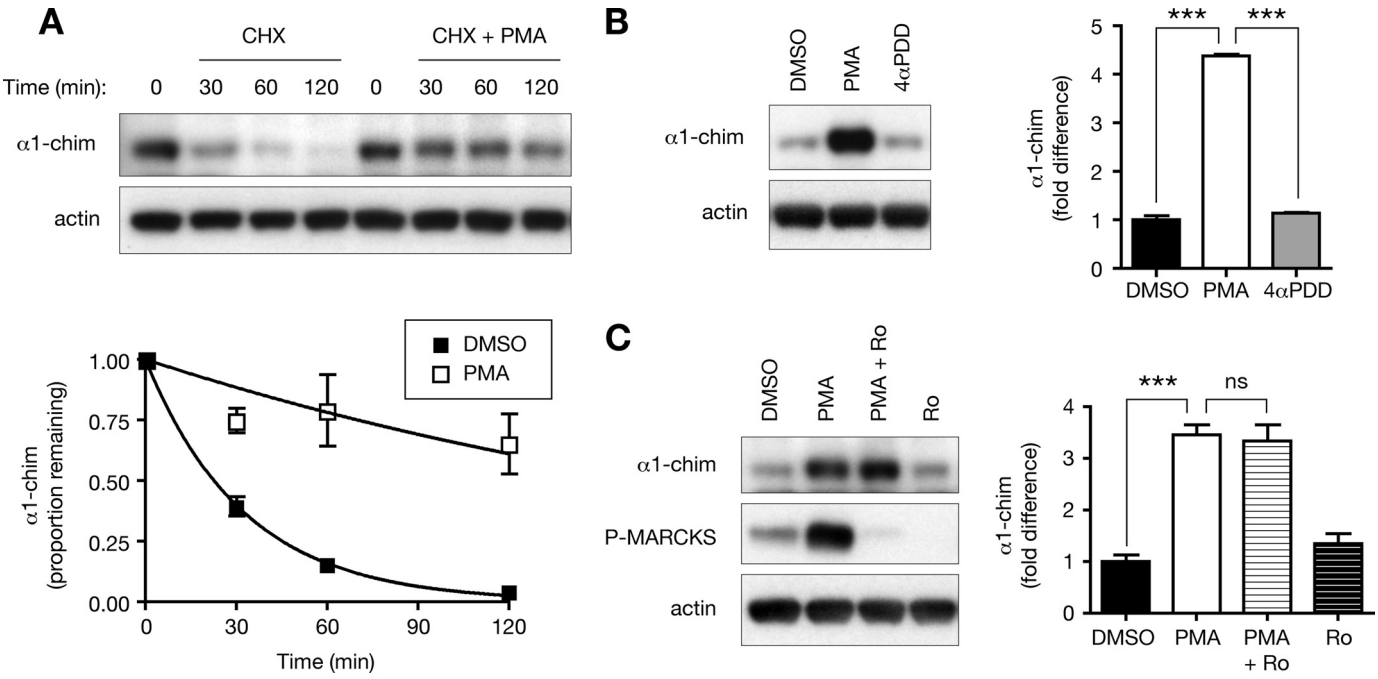

FIGURE 4. **Analysis of the influence of PMA on α1-chimaerin degradation.** *A*, cultured neurons were treated with CHX (200 μg/ml) in the presence of PMA (2 μM) or DMSO for the indicated times and then analyzed by Western blotting. *Upper panel*, representative blots; *lower panel*, densitometric analysis of α1-chimaerin abundance, expressed as a proportion of the starting levels ($n = 3$). *B*, cultured neurons were treated with the indicated phorbol esters (at 2 μM) for 2 h and analyzed by Western blotting. *Left panel*, representative blots; *right panel*, densitometric analysis of α1-chimaerin abundance, expressed as a proportion of the starting levels ($n = 3$; ***, $p < 0.001$). *4αPDD*, 4α-phorbol 12,13-didecanoate. *C*, cultured neurons pretreated with either DMSO or Ro 31-8220 (*Ro*, 2 μM) for 15 min, exposed to either DMSO or PMA (2 μM) for 2 h and then analyzed by Western blotting. *Left panel*, representative Western blots from whole cell lysates; *right panel*, densitometric analysis of α1-chimaerin abundance, expressed as a proportion of the starting levels ($n = 3$; ***, $p < 0.001$; *ns*, $p > 0.05$).

This effect shows that stabilization of α1-chimaerin by PMA requires direct binding to the C1 domain. Moreover, lack of stabilization was more pronounced in the C114A mutant compared with the P91A mutant, consistent with data showing that the loss of phorbol ester affinity is greater for C114A than P91A (28). Because both mutants were expressed from a plasmid backbone identical to that of the wild type, the differences were most likely caused by impaired PMA-mediated stabilization.

Activated Rac1 Also Causes an Accumulation of α1-Chimaerin via a Phospholipase C-dependent Mechanism—As PMA mimics DAG signaling, we next asked whether α1-chimaerin could be stabilized by endogenous DAG. We used Rac1 to generate a DAG signal, because Rac1 activation can trigger a downstream increase in PLC-β2 and PLC-γ2 activity (29). To test whether activated Rac1 has a stabilizing effect on α1-chimaerin, we transfected neurons with α1-chimaerin-HA3 in combination with EGFP-tagged Rac1 wild type or Rac1 containing T17N (dominant negative) or Q61L (constitutively active) mutations. Analysis of transfected cells as described above showed that co-expression of constitutively active Rac1 caused a 2.2-fold accumulation of tagged α1-chimaerin in comparison with EGFP alone, suggesting that activation of Rac1 could indeed stabilize α1-chimaerin (Fig. 6*A*). Importantly, the effect appeared to be specific to the activated form of Rac1, with neither wild type nor dominant negative Rac1 showing a significant change, matching the known activation dependence of Rac-PLC coupling. Because our antibodies were not specific enough to pick up the endogenous protein by immunofluorescence, we were unable to determine whether the same effect occurred with endogenously expressed α1-chimaerin.

To determine whether the stabilizing effect of active Rac1 was mediated by increased activity in the DAG signaling pathway, we used the PLC inhibitor U73122. In neurons transfected with Rac1 Q61L, incubation with U73122 caused a significant drop in the abundance of tagged α1-chimaerin, to a level similar to that in control neurons transfected with EGFP (Fig. 6*B*). This result indicates that activated Rac1 causes an accumulation of α1-chimaerin protein through a PLC- and DAG-dependent pathway, suggesting that endogenous DAG signaling, generated through activation of PLC, is capable of stabilizing α1-chimaerin against degradation in neurons.

DISCUSSION

In this study, we provide evidence that endogenous α1-chimaerin protein in neurons undergoes degradation by the proteasome and that this process is negatively regulated by phorbol ester binding, causing the protein to accumulate. Overexpression of a constitutively active mutant of Rac1 also triggered a PLC-dependent accumulation of α1-chimaerin, suggesting that the phorbol ester is mimicking a physiological action of DAG. Together these results suggest a novel regulatory mechanism that may contribute to controlling α1-chimaerin abundance, and thus its activity.

In contrast to α1-chimaerin, much progress has been made in understanding the regulation of α2- and β2-chimaerin, both of which contain an N-terminal SH2 domain. Structural

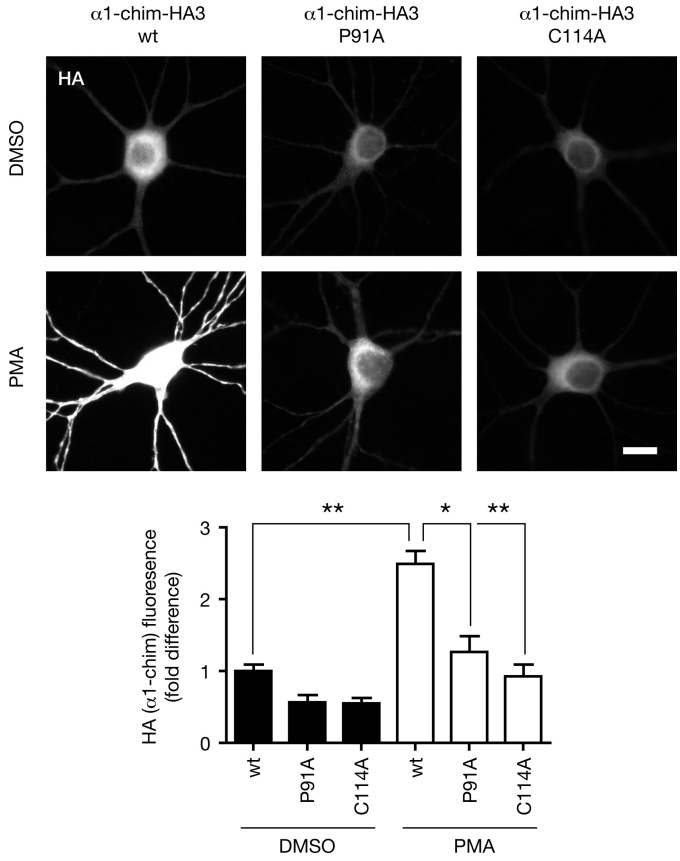

FIGURE 5. **Analysis of C1 domain point mutant stabilization by PMA.** Neurons were co-transfected with EGFP as a transfection marker and either wild type or point-mutated α1-chimaerin tagged with HA3. Cultures were treated with PMA (100 nM) or DMSO for 2 h and then fixed and immunostained. *Upper panel*, representative images of HA staining in neurons co-transfected and treated as indicated (*scale bar* = 10 μm); *lower panel*, mean HA fluorescence intensities, expressed as a proportion of the DMSO treated wild type value (20 neurons/experiment for each condition, $n = 3$ experiments; *, $p < 0.05$; **, $p < 0.01$).

data have shown that the N-terminal region in these proteins is auto-inhibitory through its occlusion of the C1 and GAP domains when the molecule is unactivated. Point mutation of the SH2 domain or truncation of the N-terminal region prevents auto-inhibition and exposes the C1 and GAP domains, creating hyperactive mutants; such mutants are able to bind DAG more avidly and inactivate Rac more readily (17–19). This finding was underscored by the recent discovery of several point mutations in the human *CHN1* gene (encoding the α-chimaerins) that destabilize the auto-inhibited conformation, leading to a form of Duane retraction syndrome in which occulomotor axon guidance is disrupted by hyper-activated α2-chimaerin (30).

Because α1-chimaerin lacks the auto-inhibitory N-terminal domain, it is likely to adopt a continuously "activated" conformation, ready to bind DAG in membranes. Brain tissue fractionation studies support this idea, with α2-chimaerin present in the cytosolic fraction, whereas α1-chimaerin is found only in a microsomal fraction (31). It therefore seems likely that alternative mechanisms exist to tightly regulate the activity of α1-chimaerin. The pathway we have described could be one such mechanism, and our demonstration that the unique N-terminal region of α1-chimaerin is involved in its instability suggests that regulated degradation may be specifically important in this isoform.

Controlled degradation could also represent a method for ensuring that active α1-chimaerin is present precisely where it is needed. Our data suggest that α1-chimaerin will be eliminated from sites where there are no appropriate signaling inputs; this will result in its activity being focused to particular subcellular structures where Rac is active. In the α2- and β2-chimaerin, isoforms such signaling specificity is achieved through SH2 binding to transmembrane receptors (8–12). However, specific binding is not excluded for α1-chimaerin, and it is likely that other mechanisms also direct its localization. For example Tmp21, a Golgi transport protein that may also associate with the presenillin complex (32), can anchor chimaerins through a protein-protein interaction with the C1 domain (33, 34).

The α1-chimaerin knockdown and overexpression phenotypes reported previously suggest that its main functional role is carried out in dendritic spines (6), and it may also interact with the synaptic glutamate receptor subunit NR2A (35). These findings suggest that α1-chimaerin is active within spines, where it may be subject to the regulated degradation we describe. Reports that the proteasome complex can shuttle into spines in response to synaptic activity (36, 37) suggest that α1-chimaerin may therefore be part of a set of proteins regulated post-translationally in this way (38). Importantly, this mechanism would also allow α1-chimaerin activity to be locally coupled to signaling within a specific spine. It will be interesting to examine whether specific PLC isoforms, or upstream partners of PLC, are important for controlling α1-chimaerin degradation via DAG and also whether any of the functional effects of those signals are relayed via α1-chimaerin.

Most substrates degraded by the proteasome are covalently tagged with polyubiquitin chains. α1-Chimaerin can also be modified in this way, although this has not yet been shown directly in neurons. The final stage of polyubiquitination is catalyzed by E3 ubiquitin ligases, a large group of molecules that recognize specific substrates and facilitate the transfer of activated ubiquitin molecules onto them (39). It is currently unknown which particular E3 ligase targets α1-chimaerin for polyubiquitination, although a number of E3 ligases have been identified that are known to affect dendritic spine structure in mammals (40–43). Inhibition of polyubiquitination by an E3 ligase may be one mechanism by which PMA and DAG block the degradation of α1-chimaerin. Because PMA is unable to stabilize α1-chimaerin carrying a point-mutated C1 domain, it seems likely that translocation or ligand binding by the C1 domain is essential for avoiding the E3 ligase action. Interestingly, the PMA-mediated stabilization of α1-chimaerin is the opposite of what is seen in the PKC family, several members of which undergo proteasomal degradation following phorbol ester stimulation (44).

We have also shown that overexpression of activated Rac1 can cause a PLC-dependent accumulation of α1-chimaerin in neurons. This is important because it indicates that DAG generated within neurons can stabilize α1-chimaerin against degradation. However, it is not currently clear whether activation

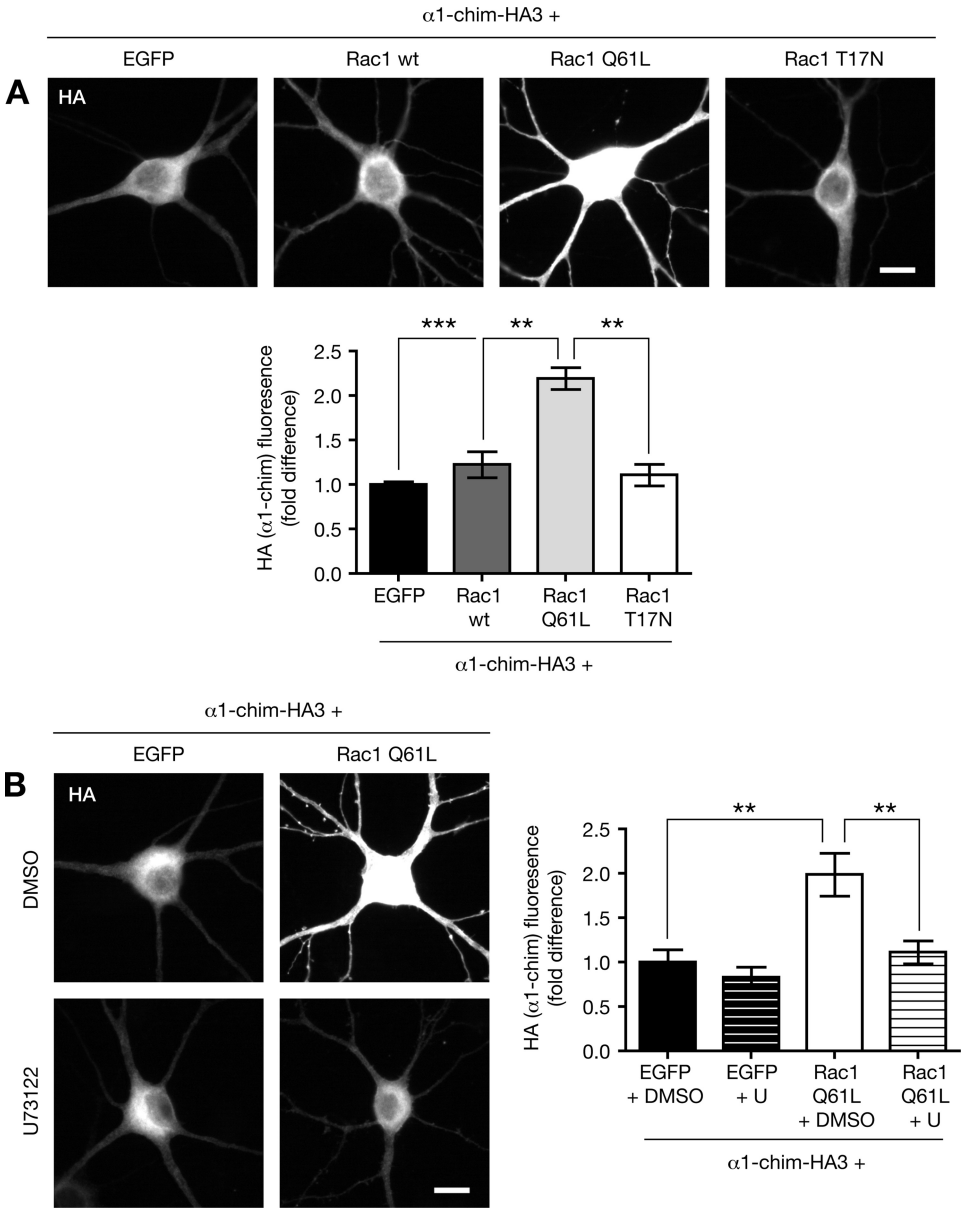

FIGURE 6. **Analysis of α1-chimaerin stabilization triggered by activated Rac1.** *A*, neurons were co-transfected with α1-chimaerin-HA3 and either wild type or point-mutated EGFP-tagged Rac1. Cultures were then fixed and immunostained. *Upper panel*, representative images of HA staining in neurons co-transfected as indicated (*scale bar,* 10 μm); *lower panel*, mean HA fluorescence intensities, expressed as a proportion of the value from EGFP co-transfected neurons (20 neurons/experiment for each condition, $n = 3$ experiments; **, $p < 0.01$; ***, $p < 0.001$). *B*, neurons were co-transfected with α1-chimaerin-HA3 and either EGFP or EGFP-tagged Rac1 Q61L. Cultures were treated with the PLC inhibitor U73122 (*U*) or DMSO for 4 h, and then fixed and immunostained. *Left panel*, representative images of HA staining in neurons co-transfected and treated as indicated (*scale bar,* 10 μm); *right panel*, mean HA fluorescence intensities, expressed as a proportion of the value from EGFP co-transfected DMSO treated neurons (20 neurons/experiment for each condition, $n = 6$ experiments; **, $p < 0.01$).

of endogenous Rac by signaling events within a neuron can cause a similar stabilization. Others have shown that β2-chimaerin translocates because of DAG signaling occurring concurrently with Rac1 activation after stimulation of the epidermal growth factor receptor, which is linked to both these signaling networks (16). Translocation in this instance was primarily due, however, to a direct coupling between the EGF receptor and PLCγ, rather than between Rac and PLC. Further work is needed to explore whether stimulation of PLC activity by Rac is the dominant physiological pathway stabilizing α1-chimaerin in neurons. If confirmed, it would lead to the interesting possibility that α1-chimaerin could take part in a generalized negative feedback loop to constrain Rac activity, becoming locally stabilized in areas of increased Rac activation.

In our previous work, we found that both knockdown and overexpression of α1-chimaerin was sufficient to alter the density and morphology of mature dendritic spines in neurons (6). Accurate control of α1-chimaerin protein levels is therefore critical for maintaining the structure of mature spines, which can be stable over long periods in cortical regions of the adult brain (45). Our current findings define a new pathway by which this regulation of α1-chimaerin levels may be achieved, and it will be interesting in the future to de-

termine whether dysregulation of α1-chimaerin expression levels is involved in the pathogenesis of neurological problems such as Alzheimer disease, where spine structure and density are affected (46).

Acknowledgments—We thank Peter Scheiffele and Mark Philips for contributing important reagents and Aviva Tolkovsky for helpful advice throughout this project.

REFERENCES

1. Alvarez, V. A., and Sabatini, B. L. (2007) *Annu. Rev. Neurosci.* **30,** 79–97
2. Cingolani, L. A., and Goda, Y. (2008) *Nat. Rev. Neurosci.* **9,** 344–356
3. Jaffe, A. B., and Hall, A. (2005) *Annu. Rev. Cell Dev. Biol.* **21,** 247–269
4. Tashiro, A., and Yuste, R. (2004) *Mol. Cell. Neurosci.* **26,** 429–440
5. Nakayama, A. Y., Harms, M. B., and Luo, L. (2000) *J. Neurosci.* **20,** 5329–5338
6. Buttery, P., Beg, A. A., Chih, B., Broder, A., Mason, C. A., and Scheiffele, P. (2006) *Proc. Natl. Acad. Sci. U.S.A.* **103,** 1924–1929
7. Yang, C., and Kazanietz, M. G. (2007) *Biochem. J.* **403,** 1–12
8. Takeuchi, S., Yamaki, N., Iwasato, T., Negishi, M., and Katoh, H. (2009) *FEBS Lett.* **583,** 1237–1242
9. Wegmeyer, H., Egea, J., Rabe, N., Gezelius, H., Filosa, A., Enjin, A., Varoqueaux, F., Deininger, K., Schnütgen, F., Brose, N., Klein, R., Kullander, K., and Betz, A. (2007) *Neuron* **55,** 756–767
10. Shi, L., Fu, W. Y., Hung, K. W., Porchetta, C., Hall, C., Fu, A. K., and Ip, N. Y. (2007) *Proc. Natl. Acad. Sci. U.S.A.* **104,** 16347–16352
11. Iwasato, T., Katoh, H., Nishimaru, H., Ishikawa, Y., Inoue, H., Saito, Y. M., Ando, R., Iwama, M., Takahashi, R., Negishi, M., and Itohara, S. (2007) *Cell* **130,** 742–753
12. Beg, A. A., Sommer, J. E., Martin, J. H., and Scheiffele, P. (2007) *Neuron* **55,** 768–778
13. Caloca, M. J., Wang, H., and Kazanietz, M. G. (2003) *Biochem. J.* **375,** 313–321
14. Manser, E., Leung, T., Monfries, C., Teo, M., Hall, C., and Lim, L. (1992) *J. Biol. Chem.* **267,** 16025–16028
15. Colón-González, F., and Kazanietz, M. G. (2006) *Biochim. Biophys. Acta* **1761,** 827–837
16. Wang, H., Yang, C., Leskow, F. C., Sun, J., Canagarajah, B., Hurley, J. H., and Kazanietz, M. G. (2006) *EMBO J.* **25,** 2062–2074
17. Sosa, M. S., Lewin, N. E., Choi, S. H., Blumberg, P. M., and Kazanietz, M. G. (2009) *Biochemistry* **48,** 8171–8178
18. Colón-González, F., Leskow, F. C., and Kazanietz, M. G. (2008) *J. Biol. Chem.* **283,** 35247–35257
19. Canagarajah, B., Leskow, F. C., Ho, J. Y., Mischak, H., Saidi, L. F., Kazanietz, M. G., and Hurley, J. H. (2004) *Cell* **119,** 407–418
20. Brewer, G. J., Torricelli, J. R., Evege, E. K., and Price, P. J. (1993) *J. Neurosci. Res.* **35,** 567–576
21. Michaelson, D., Abidi, W., Guardavaccaro, D., Zhou, M., Ahearn, I., Pagano, M., and Philips, M. R. (2008) *J. Cell Biol.* **181,** 485–496
22. Michaelson, D., Silletti, J., Murphy, G., D'Eustachio, P., Rush, M., and Philips, M. R. (2001) *J. Cell Biol.* **152,** 111–126
23. Storm, E. E., Rubenstein, J. L., and Martin, G. R. (2003) *Proc. Natl. Acad. Sci. U.S.A.* **100,** 1757–1762
24. Niwa, H., Yamamura, K., and Miyazaki, J. (1991) *Gene* **108,** 193–199
25. Lennon, G., Auffray, C., Polymeropoulos, M., and Soares, M. B. (1996) *Genomics* **33,** 151–152
26. Graham, D. R., Garnham, C. P., Fu, Q., Robbins, J., and Van Eyk, J. E. (2005) *Proteomics* **5,** 2309–2314
27. Arbuzova, A., Schmitz, A. A., and Vergères, G. (2002) *Biochem. J.* **362,** 1–12
28. Kazanietz, M. G., Wang, S., Milne, G. W., Lewin, N. E., Liu, H. L., and Blumberg, P. M. (1995) *J. Biol. Chem.* **270,** 21852–21859
29. Harden, T. K., Hicks, S. N., and Sondek, J. (2009) *J. Lipid Res.* **50,** S243–S248
30. Miyake, N., Chilton, J., Psatha, M., Cheng, L., Andrews, C., Chan, W. M., Law, K., Crosier, M., Lindsay, S., Cheung, M., Allen, J., Gutowski, N. J., Ellard, S., Young, E., Iannaccone, A., Appukuttan, B., Stout, J. T., Christiansen, S., Ciccarelli, M. L., Baldi, A., Campioni, M., Zenteno, J. C., Davenport, D., Mariani, L. E., Sahin, M., Guthrie, S., and Engle, E. C. (2008) *Science* **321,** 839–843
31. Hall, C., Michael, G. J., Cann, N., Ferrari, G., Teo, M., Jacobs, T., Monfries, C., and Lim, L. (2001) *J. Neurosci.* **21,** 5191–5202
32. Chen, F., Hasegawa, H., Schmitt-Ulms, G., Kawarai, T., Bohm, C., Katayama, T., Gu, Y., Sanjo, N., Glista, M., Rogaeva, E., Wakutani, Y., Pardossi-Piquard, R., Ruan, X., Tandon, A., Checler, F., Marambaud, P., Hansen, K., Westaway, D., St George-Hyslop, P., and Fraser, P. (2006) *Nature* **440,** 1208–1212
33. Wang, H., and Kazanietz, M. G. (2010) *Mol. Biol. Cell* **21,** 1398–1408
34. Wang, H., and Kazanietz, M. G. (2002) *J. Biol. Chem.* **277,** 4541–4550
35. Van de Ven, T. J., VanDongen, H. M., and VanDongen, A. M. (2005) *J. Neurosci.* **25,** 9488–9496
36. Bingol, B., Wang, C. F., Arnott, D., Cheng, D., Peng, J., and Sheng, M. (2010) *Cell* **140,** 567–578
37. Bingol, B., and Schuman, E. M. (2006) *Nature* **441,** 1144–1148
38. Ehlers, M. D. (2003) *Nat. Neurosci.* **6,** 231–242
39. Pickart, C. M., and Eddins, M. J. (2004) *Biochim. Biophys. Acta* **1695,** 55–72
40. Kawabe, H., Neeb, A., Dimova, K., Young, S. M., Jr., Takeda, M., Katsurabayashi, S., Mitkovski, M., Malakhova, O. A., Zhang, D. E., Umikawa, M., Kariya, K., Goebbels, S., Nave, K. A., Rosenmund, C., Jahn, O., Rhee, J., and Brose, N. (2010) *Neuron* **65,** 358–372
41. Hung, A. Y., Sung, C. C., Brito, I. L., and Sheng, M. (2010) *PLoS One* **5,** e9842
42. Dindot, S. V., Antalffy, B. A., Bhattacharjee, M. B., and Beaudet, A. L. (2008) *Hum. Mol. Genet.* **17,** 111–118
43. Ang, X. L., Seeburg, D. P., Sheng, M., and Harper, J. W. (2008) *J. Biol. Chem.* **283,** 29424–29432
44. Lu, Z., Liu, D., Hornia, A., Devonish, W., Pagano, M., and Foster, D. A. (1998) *Mol. Cell. Biol.* **18,** 839–845
45. Holtmaat, A. J., Trachtenberg, J. T., Wilbrecht, L., Shepherd, G. M., Zhang, X., Knott, G. W., and Svoboda, K. (2005) *Neuron* **45,** 279–291
46. Knobloch, M., and Mansuy, I. M. (2008) *Mol. Neurobiol.* **37,** 73–82